IMPROVING THE ROBUSTNESS OF TURBULENT FLUXES: AN EXAMINATION OF THE ROLE OF WAVES ON FLUXES AND TURBULENCE STATISTICS

by

JASMINE VICTORIA VANEXEL

(Under the Direction of Monique Leclerc)

ABSTRACT

Gravity waves and turbulence are often intermixed throughout the stable boundary layer and together they play an integral role in atmospheric dynamics. This work focuses on wave and wave-like disturbances and their impact on the nocturnal boundary layer turbulence and turbulent fluxes. The data was collected from a 450m tall tower at the Savannah River Site in Aiken, South Carolina. Wave events were selected to adequately evaluate the wave enhancement of turbulence in winter and summer seasons at different measurement heights. Results suggest seasonality in the frequency of waves near the ground and their impact on turbulence statistics. For the range of periods studied, the impact varies as much as 55% in the turbulent kinetic energy values though on average, the impact of the errors is more modest and the impact of waves on scalar fluxes such as carbon dioxide and water vapor is small.

INDEX WORDS: Turbulence, gravity waves, nocturnal boundary layer, stable boundary layer, eddy-covariance, turbulent fluxes, turbulence statistics

IMPROVING THE ROBUSTNESS OF TURBULENT FLUXES: AN EXAMINATION OF THE ROLE OF WAVES ON FLUXES AND TURBULENCE STATISTICS

By

JASMINE VICTORIA VANEXEL

B.S., Paine College, 2011

A Thesis Submitted to the Graduate Faculty of The University of Georgia in Partial Fulfillment of the Requirements for the Degree

MASTER OF SCIENCE

ATHENS, GEORGIA

2014

IMPROVING THE ROBUSTNESS OF TURBULENT FLUXES: AN EXAMINATION OF THE ROLE OF WAVES ON FLUXES AND TURBULENCE STATISTICS

by

JASMINE VICTORIA VANEXEL

Major Professor: Monique Leclerc

Committee: David Stooksbury
Ian Flitcroft

Electronic Version Approved:

Julie Coffield
Interim Dean of the Graduate School
The University of Georgia
August 2014

ACKNOWLEDGEMENTS

I would like to thank God first and foremost for giving me the focus and diligence to complete this thesis. Nothing is possible without God.

I want to thank Professor Monique Leclerc for her guidance, support, and unwavering faith in my abilities to complete this thesis. I truly believe that I have gained so much knowledge in research, presentation, and writing through working with this wonderful woman and brilliant scientist. I thank her for giving me the opportunity to work with her and the group.

Thank you to David Durden, for lending his programs, time, and incite to help me complete this thesis, which is a continuation of his master's research. I could not have started or completed this process without his willingness to listen to my ideas and help me to work out any details and/or problems.

Dr. Henrique Duarte, thank you for diligently teaching me Linux commands and Fortran 90/95 and teaching me advanced programing. Drs. Gengsheng Zhang and David Cotton I thank for their input and help debugging early data and programing errors.

To my committee members, Dr. David Stooksbury and Dr. Ian Flitcroft, I thank you both for your patience, encouragement, advice and guidance in writing this thesis. I appreciate your willingness to offer your time and input over the last few years.

I would like to thank Dr. Gerald Arkin for introducing me to Professor Leclerc and the group and always being an advocate for me.

Last but certainly not least, I would like to thank my mom, Janice McGhee, and sister, Siara, for being my support system and occasionally my comic relief. You two are the wind beneath my wings.

TABLE OF CONTENTS

LIST OF TABLES

LIST OF FIGURES

1 INTRODUCTION

The present study evaluates some of the mechanisms that lead to errors in fluxes and turbulence measurements. That is important since the measurements of gaseous emissions have large uncertainties. Due to turbulence generated by wind shear and atmospheric instability, measuring fluxes in the stable nocturnal boundary layer is often characterized with numerous challenges. Turbulent events that include internal gravity waves, “submeso” motions, bores, and advection (Mahrt, 2009; Nappo et al., 2008), lead to flux and turbulence statistics errors, and are common in the stable nighttime boundary layer. The present study evaluates the degree to which one of these features contributes to errors in the exchange of gases and energy over two contrasting seasons and at different levels from the ground for the first time in a quasi-climatological sense.

Uncertainties are largest in nighttime conditions. This is because the stable nocturnal boundary layer often has within it a mixture of intermittent turbulence, waves and other phenomena. With stronger winds and weaker surface cooling there may be continuous turbulence as in the case of daytime conditions, or on occasion during the night. In contrast, intermittent turbulence occurs during clear sky nights with weak winds and/or advection of warm air over a cooler surface and is often present at night. Although turbulence is typically intermittent in substantially stable conditions, intermittency has been observed in weakly stable conditions (Mahrt 2009).

The preferred method used to measure turbulent fluxes within the atmosphere is the eddy-covariance method. The eddy-covariance technique measures fluxes of momentum and scalars under well mixed convective boundary-layer conditions. The method is accurate, direct, and deceptively simple and has widely been used in agriculture (Mathieu et al., 2005). However, the inability to measure net ecosystem exchange accurately in the stable nocturnal boundary layer has been reported (Karipot et al., 2006; Mahrt, 2009; Mathieu et al., 2005; Van Gorsel et al., 2011). Specifically, the potential problems and uncertainties surrounding the calculation of turbulence statistics and fluxes in the presence of gravity waves and other wave activity are yet to be fully understood and resolved (Durden et al., 2013; Van Gorsel et al., 2011).

Gravity waves, also known as buoyancy waves, result from harmonic oscillations of fluid particles caused by buoyancy (Nappo, 2002). Such waves exist due to the stability and density stratification of the atmosphere. They transport energy and can overturn and generate their own turbulence. These effects can be detected as fluctuations of pressure, temperature, reflectivity, and the refractive index (Sorbjan and Czerwinska, 2013; Nappo, 2002). Breaking gravity waves, in particular, are often associated with intermittent turbulence in the stable boundary layer (Chimonas, 1985; Finnigan, 1988; Lee et. al., 1996). Throughout the night, turbulence undergoes a significant change in character during the convective to stable condition transition. The nighttime boundary layer is also shallower than the daytime boundary layer, which will result in differences in turbulence and waves. In the stable boundary layer, gravity wave frequencies and the frequencies of the energy-containing turbulence eddies are similar (Finnigan, 1988, 1999; Viana et al., 2009). Thus, wave energy can be confused with turbulence energy resulting in the errors in second-order turbulence quantities such as fluxes and turbulent kinetic energy. In general, waves are ubiquitous in the atmosphere.

Wave-like motions have been detected and found to be associated with thermal instabilities at the surface and downward transport of momentum (Sun et al., 2004). Wave and turbulence events observed in the stable boundary layer produce mixing of energy and temperature and CO_2 scalars and contribute to horizontal and vertical fluxes (Viana et al., 2009; Van Gorsel et al., 2011; Zeri and Sa, 2011; Durden et al., 2013). Einaudi and Finnigan (1993) detail two winter events of wave-turbulence interaction in the stably stratified boundary layer, in which the transfer of kinetic energy from wave to turbulence, they thought was very likely to be a typical occurrence. When waves are generated above the turbulent boundary layer, they can maintain a constant amplitude over a long period, up to several tens of wave periods (Einaudi and Finnigan, 1993). Ducted waves are bound between the ground surface and some atmospheric reflecting layer above (Cooper et al., 2006; Fritts et al., 2003; Newsom and Banta, 2003; Rees et al., 1988), thus producing a wave guide allowing propagation to occur over long distances and time periods. When this occurs, the wave may be more easily distinguishable from turbulence. It is thus necessary to further characterize the interaction of turbulence and large-amplitude wave and wave-like events on a larger scale and long term in the stable nocturnal boundary layer. This wave-turbulence interaction acts as an interchange of energy between the wave and turbulent fields, and is responsible for maintaining the turbulent field, particularly at times of light winds and Richardson numbers in the very stable boundary layer that are large and positive (Einaudi and Finnigan, 1993).

Previous studies have thoroughly interpreted cases over a few days (Einaudi and Finnigan, 1993; Van Gorsel et al., 2011; Durden et al., 2013), but a greater understanding of wave-turbulence interactions at a seasonal scale could provide additional insight into the interpretation of eddy-covariance measurements. Van Gorsel et al., (2011) analyzed exchange within and above the canopy and the effect of gravity waves on it. Several other studies have looked at gravity wave impact on atmospheric flow within and above the canopy (Einaudi and Finnigan, 1993; Nappo et al., 2008; Viana et al., 2009; Van Gorsel et al., 2011; Zeri and Sa, 2011; Durden et al., 2013).

Durden et al. (2013), in a preliminary study, specifically looked at the gravity wave impact on turbulence statistics and turbulent fluxes as a function of measurement height. They used both eddy-covariance and microbarograph data for their analysis. With only a very small dataset, the results show potential and pointed the way to the need for a more exhaustive, more robust study based on more nights, and in contrasting seasons. In their study, they found that wave-like activity can impact turbulence statistics by up to 50% and fluxes upwards of 10% for CO_2 depending on the averaging time (Durden et al., 2013). They did not consider the impact of different threshold criteria in the pressure perturbations, a variable that can influence the results.

The purpose of this research is thus to present a quasi-climatological study of wave frequency and periods and their impact on nighttime wave-modified turbulence and fluxes measured on a 450m tall tower above a forest canopy. This research jointly examines the characteristics of nocturnal boundary layer turbulence influenced by gravity waves during the winter and summer. Thermal inversions are strongest in the winter, when there are clear skies and/or snow. We thus expect wave-turbulence interaction to be modulated with season. The variations of these wave events across seasons were considered. There are two objectives: 1) Evaluate for the first time the frequency and impact of these disturbances on the eddy-flux method results for contrasting seasons 2. Evaluate, using a comprehensive database spanning 151 nights the level of errors contributed by wavelike disturbances in turbulence statistics and turbulent fluxes as a function of height within the boundary layer.

2 SITE AND MEASUREMENTS

The turbulence data was collected during an ongoing experiment conducted at a 450 m tall TV tower near Beech Island, SC (33°24'21''N 81°50'02''W) at the Savannah River site (Figure 2.1). The tower is positioned on a rural ridge at an elevation of ~116m, with eddy-covariance systems at 33.5, 68, and 329m above ground level. This location is within a mixed use agricultural (pine forest and field crops), residential, and industrial zone. Each eddy-flux system (Figure 2.2) consists of a fast-response omnidirectional three-dimensional sonic anemometer (Applied Technologies, Inc., Longmont, CO models, Sx (34 m level) and A (68 and 329 m levels)) and a fast-response open path CO_2/H_2O gas analyzer (Li-Cor Biosciences, Lincoln, NE, Model 7500). Measurements were collected at 10 Hz. Data including three-velocity components, sonic temperature, and H_2O and CO_2 concentrations were sampled and logged with two CR3000 data loggers (Campbell Scientific Inc., Logan, UT).

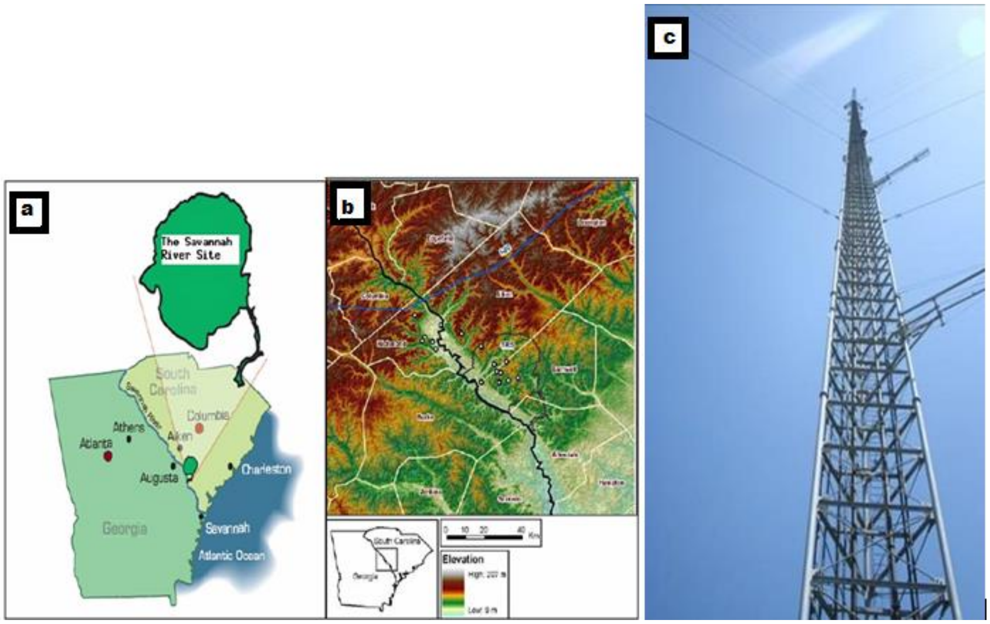

Figure 2.1: (a) General location of Savannah River site (b) satellite aerial view of the site and (c) 450 meter tall tower (Courtesy of Natchaya Pingintha).

Figure 2.2 (a) Eddy-flux system including a sonic anemometer and a fast-response open-path CO_2/H_2O gas analyzer and (b) a single microbarograph.

Surface pressure was measured via an array of six microbarographs (Model 270, Setra Systems, Boxborough, MA) configured in two concentric equilateral triangles with 100-m and 300-m sides near the ground adjacent to the tall tower. A microbarograph with static pressure disks was used to measure static atmospheric pressure at the surface. This surface pressure is a good indication of the wave behavior near the critical level (Einaudi and Finnigan, 1981). The pressure transducer continuously collected data at 20 Hz to a data logger (model CR5000) located at the base of the tall tower. The data were averaged to 0.1 Hz to be used in the wavelet analysis.

3 METHODOLOGY

The variation of the wave signal and the impact on turbulence fluxes was analyzed from the data from the eddy-covariance systems at different measurement heights on the tall tower (34, 68, and 329m). This thesis examines data collected from June 1 to August 31, 2009 and December 1, 2009 to February 28, 2010 with consideration of the time of night between midnight (0000 EST) and 6 AM (0600 EST). There was no data for July available for this study due to instrumentation malfunctioning and subsequent repair, so a total of 151 days were considered. Next, the data was filtered based on quality. In this regard, any erroneous data due to inclement weather was excluded and spiking in the pressure signals was detected and removed from the data selected. From the remaining data, each day was analyzed for any wave and wave-like events, the wave periods corresponding to each event between 3 and 30 minutes, and the measurement height of wave and wave-like activity within the nocturnal boundary layer. Periods between 3 and 30 minutes was used to selectively identify the wave events thought to be most likely to significantly influence the turbulence of each night. The lower limit of periods was 3 minutes; however, the maximum period of 30 minutes is the standard time used for flux calculations (Nappo, 2002). The averaging time chosen was 30 minutes because it is by far the most widely used standard period of flux calculations (Viana et al., 2012; Nappo, 2008; Zeri and Sa, 2011).

Wave frequency (or number of wave events per night) in relation to the corresponding period and the measurement height of detection were identified. The wave frequency was particularly a factor for comparison between summer and winter nights. On any particular night, a large-amplitude wave event could occur. A space-time representation of the wave energy density was created and analyzed in terms of both its period and duration. Provided it fulfilled the above-mentioned criteria, it was then used for further analysis.

3.1 WAVE DETECTION

To evaluate the role of waves on turbulence calculations, a separation of the wave from the turbulence component must be done. The method applied by Hauf et al. (1996) and Nappo et al. (2008) using a band-pass filter to separate waves from turbulence was employed. The standard deviation of the pressure (σ_p) was calculated, using the residual signal output from the bandpass filter, and used to determine a detection threshold for large amplitude events (Durden et al., 2013). Unlike the latter study, both $2\sigma_p$ and $3\sigma_p$ detection thresholds were used in this study as it is a factor that modulates the wave detection level and hence, the number of waves detected. The days of good quality were bandpass filtered and 65 of those nights had waves with large amplitudes (using $2\sigma_p$). A wave analysis was performed on the detected signal to identify the time, period, and duration of the wave event after differentiating the turbulence and the wave components of a raw signal.

Richardson (Ri) numbers are parameters typically used to characterize the degree of atmospheric stability. They give a ratio of the buoyancy to shear. In the present study, the flux Richardson number, Ri_f, was used to characterize each night used in this analysis. Intermittency, on the global scale, corresponds to an increase in Ri number to quantities exceeding the critical level when there is vertical mixing (Mahrt, 1999). This leads to a degeneration of turbulence versus regeneration. Another form of the Richardson number, applied over a finite layer, is the Bulk Richardson number, Ri_b. For sake of completeness, we also include the values for the Ri_b for the reader. We have characterized each night using a Ri_f. The bulk Ri number was calculated using the 68 and 329m levels. Ultimately, the 68m level was only used to derive the stability parameter because of the close proximity to the 34m level. Typically, a Ri_b value between 0.1 and 10 is indicative of a high degree of turbulence, and thus a weakly stable boundary layer. A range of 10-45 is stable, and values greater than 50 suggest a deeply stratified atmosphere with minimal to no turbulence.

3.2 WAVE ANALYSIS

Wavelet analysis is a tool used to analyze atmospheric wave signals, i.e. gravity waves. It is accomplished using a decomposition of the components of a signal and band-pass filtering at different frequencies, while retaining information in the time domain (Torrence and Compo, 1998). In recent years, wavelet analysis has been used in the study of turbulence fluxes, coherent structures and motions, and wave-modified turbulence (Farge, 1992; Collineau and Brunet, 1993a, b; Turner and Leclerc, 1994; Turner et al., 1994; Salmond, 2005; Zhang et al., 2007; Zhu et al., 2010). This analysis is utilized for assessing waves as a function of period, amplitude, and duration of wave event within the atmospheric boundary layer, the wavelet analysis is particularly effective when intermittency is present within a signal (Farge, 1992; Collineau and Brunet, 1993a, b; Turner and Leclerc, 1994; Turner et al., 1994). This study is ideal for wavelet analysis such as this one where the waves and turbulence present are highly intermittent. The Morlet wavelet was chosen for its high resolution in frequency space, which is instrumental in accurately determining the period and frequency range of the wave events (Nappo, 2002; Torrence and Compo, 1998). The selected pressure data was bandpass filtered. First, wavelets were identified through periods of wave-like activity. This was done in four-hour windows, a timeframe first used by Nappo et al. (2008) which enables for a long wave event or several shorter waves to propagate. Next, the wave signal was band-pass filtered to estimate the amplitude of perturbations of wind components, temperature, and water vapor. These wave perturbations were then removed from the original time series. The resulting time series then had linear trends removed and was decomposed into frequency components through wavelet analysis. Using the triple decomposition method applied by Einaudi and Finnigan (1981, 1993) we distinguished the original and 'dewaved' flux. The decomposition was first introduced by Hussein and Reynolds (1972) to separate a wave signal into three components: the mean, turbulence, and wave. The original unfiltered signal in which a wave is present is referred to as the original turbulent flux signal. Therefore, a Hussein decomposition of a given variable $u(z,t)$ is performed using the equation:

$$u(z,t) = \bar{u}(z) + u'(z,t) + u(z,t) \tag{1}$$

where the variables on the right represent the mean or background component, turbulence which does not belong to mean and is not locked in phase with the primary wave, and wave component, which is assumed to be initiated by shear instability process of the troposphere above the boundary layer, respectively. With this partitioning, the contribution from each component can now be assessed.

Phase averaging is a technique used to separate wave and turbulence and 'typically' ten wave periods are required to perform a successful phase average (Einaudi and Finnigan, 1993). However, since these successive periods are rare, the aforementioned method is the better option for decomposition. If the wave component is not removed, then the flux would be:

$$\overline{w'u'}^{original} = \overline{(w - w')(u - u')} \tag{2}$$

Using the triple decomposition, the vertical flux of the variable, u, is given by:

$$\overline{w'u'}^{corrected} = \overline{(w - \bar{w} - \tilde{w})(u - \bar{u} - \tilde{u})} \tag{3}$$

where Equation 5 is the turbulent flux of with the wave component removed taken to be the flux Reynolds flux (Webb, Pearman, and Leuning, 1980). This study does not detail the impact of wave(s) on the total flux, only the turbulent flux. Following the decomposition of the unfiltered signal for each night, nights were assessed based on atmospheric stability, the number of waves, the intensity of waves, and the average period of waves occurring within a six-hour window between midnight and 0600 EST.

4 RESULTS

For the months of June 2009 and August 2009 (July data was not included), using a detection threshold of three standard deviations for large amplitude events, sixteen nights were considered to have large amplitude events. The two sets of vertical lines in the pressure signal graphs represent the 2 and $3\sigma_p$ detection thresholds (see Figure 4.1). Following the wavelet transformation, a total of ten nights were both large amplitude nights and showed high wavelet energy density in a space-time representation. These representations (see Figure 4.2) depict the time of day in hours, and wave period in minutes, and the wavelet energy density.

For the period December 2009 to February 2010, 28 nights had large amplitude pressure signals (fourteen nights in December alone). Twelve of these nights in the winter months had wave or wave-like events occur, had large amplitudes, and high energy density. The two seasons, summer and winter, varied in the amount of waves, the intensity of the wave(s), and stability (based on the Richardson number). The static pressure data exhibited a lot of day to day variability and because there were a large number of nights, the analysis was limited to three nights from each season to represent the differences found within each season and to reduce redundancy in the results. For the summer months, the pressure time series (see Figures 4.1, 4.3, 4.5, 4.7) were smaller (less than or equal to 0.1mb) and thus the scale of the wave energy density (see Figures 4.2, 4.4, 4.6, 4.8) showed a smaller scale (less than 1 J/m^3). For the winter months, the highest pressures were larger than those in the summer (greater than 1mb) and as a result the scale of the wave energy density was larger (greater than 1 and up to 45 J/m^3).

In Figures 4.1 through 4.8, the pressure signals and wave energy/period plots are depicted for the four nights selected. June 8th has a Ri_b of 39.59, the static pressure is as high as 0.07mb, but because this was at the end of the time window this wave event could not be analyzed. Two events (see Figure 4.1), one at 2am and another at ~4:30am, corresponded to pressures of ~0.05 and ~0.04mb respectively. However, the intensity of the wave at 4:30 is very small and the duration is short (see Figure 4.2). This wave would not be used to correct the statistics and turbulent fluxes; instead, the wave at 2am with a period of ~16 min and a longer duration would be selected. When any night has multiple wave events, the wave selected is that with the greatest intensity, largest period, or a combination of any of these criteria.

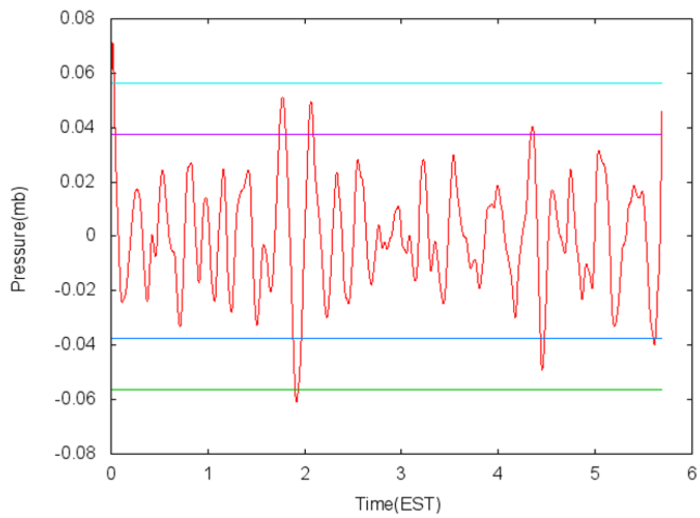

Figure 4.1 Static pressure for June 8, 2009 showing activity from 0000-0600 EST and the 2 σ_p (two inner horizontal lines) and 3 (two outer horizontal lines) σ_p detection threshold lines.

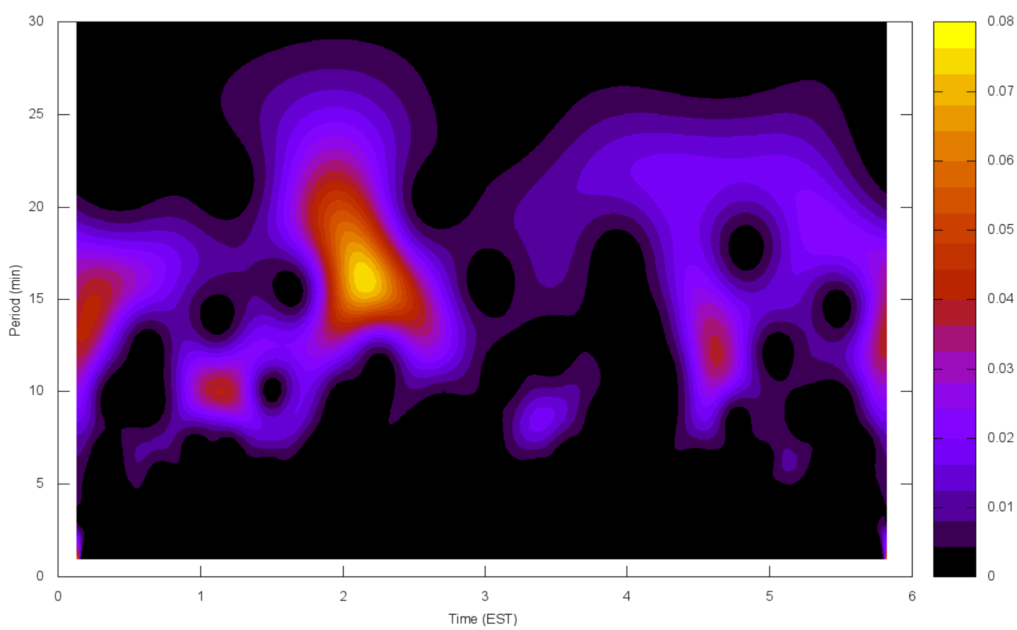

Figure 4.2 Wave-like activity from 0000-0600 EST, period (in minutes) and wave energy density (J/m^3) for June 8, 2009.

August 12th had a large pressure of ~0.08mb at approximately 4:50am (see Figure 4.3). This signal corresponded to an event with an energy density of ~0.25 J/m^3 with a period of 12 min (Figure 4.4). This night represents the highest intensity of the activity seen for the summer months and with a Ri_b of 4.11, the night is less stable than June 8th. Considering the bulk Richardson numbers for June 8th and August 12th, more wave activity with a higher energy density and perhaps longer periods would be expected. However, the difference in stability only appears to be apparent in the length of the period for the single wave event occurring during each morning.

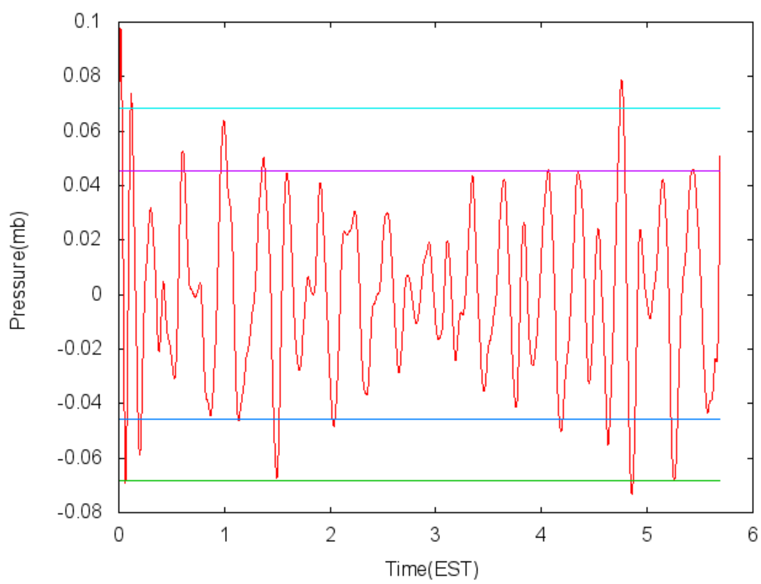

Figure 4.3 Static pressure for August 12, 2009 showing activity from 0000-0600 EST and the 2 σ_p (two inner horizontal lines) and 3 (two outer horizontal lines) σ_p detection threshold lines.

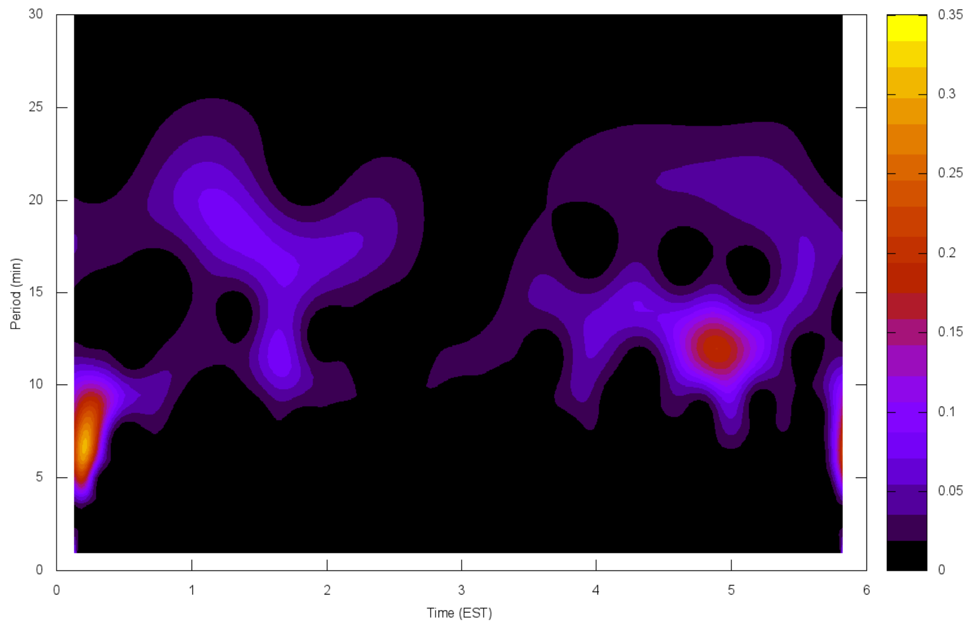

Figure 4.4 Wave-like activity from 0000-0600 EST, period (in minutes) and wave energy density (J/m^3) for August 12, 2009.

On January 2nd, two events cause pressure spikes of more than 0.15 (Figure 4.5), at the time of the disturbances the Ri_b was 3.7. This instability resulted in a wave with an energy density of ~0.5 and periods of approximately 17 and 20 minutes (Figure 4.6). January 25th was a mildly stable night with a Ri_b of 40.2. The pressure on this night was higher than any previous night. The signal exceeded the 2 and 3σ_p detection threshold throughout the six-hour window (Figure 4.7), with a maximum pressure of ~0.7 at approximately 4am. The scale for the pressure perturbations is extremely high (Figure 4.8). Summarizing, the average wave periods and durations of these selected episodes was 16 min from 01:00 to 03:00 on June 8, 2009, 12 min from 03:45 to 05:45 on August 12, 2009, 19 min from 01:00 to 03:00 on January 2, 2010, and 11.3 min from 03:45 to 05:45 on January 25, 2010. Overall, the pressure perturbations were greater (more intense) during the winter than the summer, although the periods were shorter.

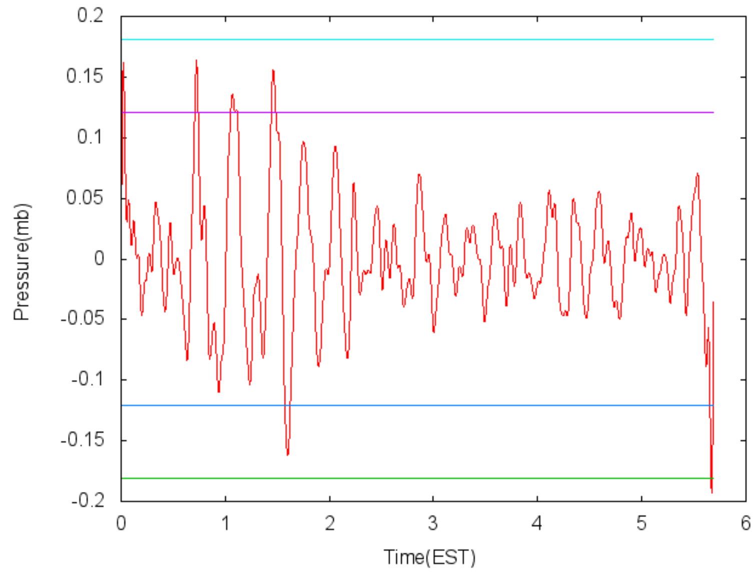

Figure 4.5 Static pressure for January 2, 2010 showing activity from 0000-0600 EST and the 2 σ_p (two inner horizontal lines) and 3 (two outer horizontal lines) σ_p detection threshold lines.

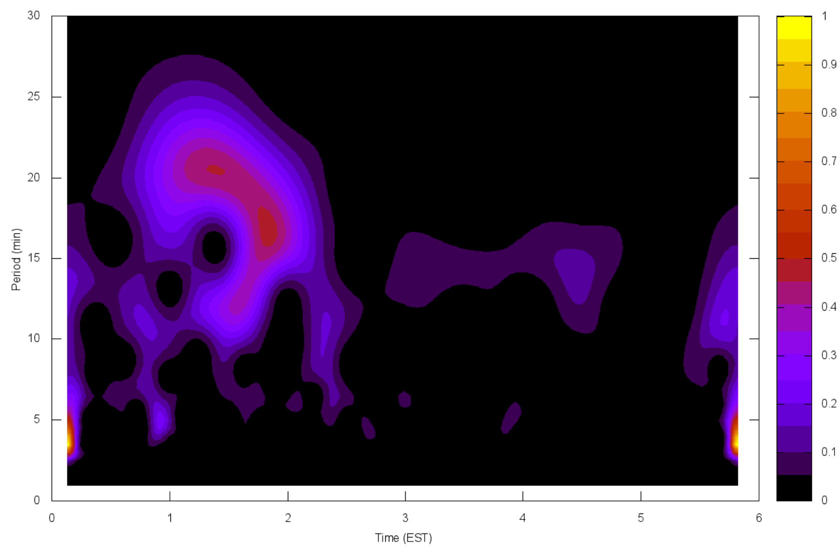

Figure 4.6 Wave-like activity from 0000-0600 EST, period (in minutes) and wave energy density (J/m^3) for January 2, 2010.

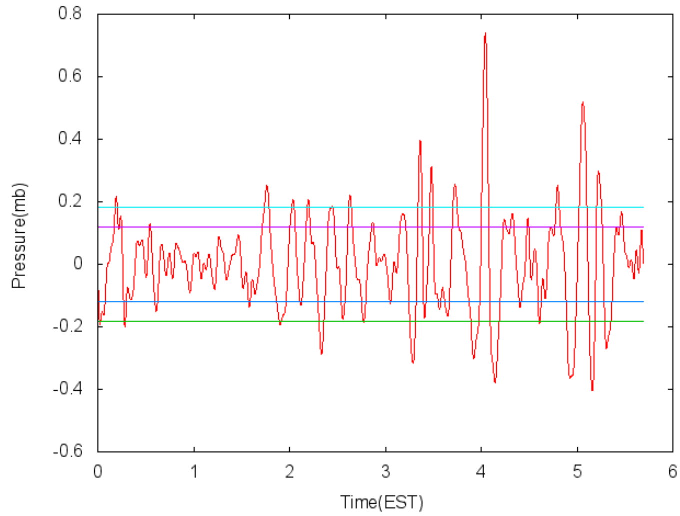

Figure 4.7 Static pressure for January 25, 2010 showing activity from 0000-0600 EST and the 2 σ_p (two inner horizontal lines) and 3 (two outer horizontal lines) σ_p detection threshold lines.

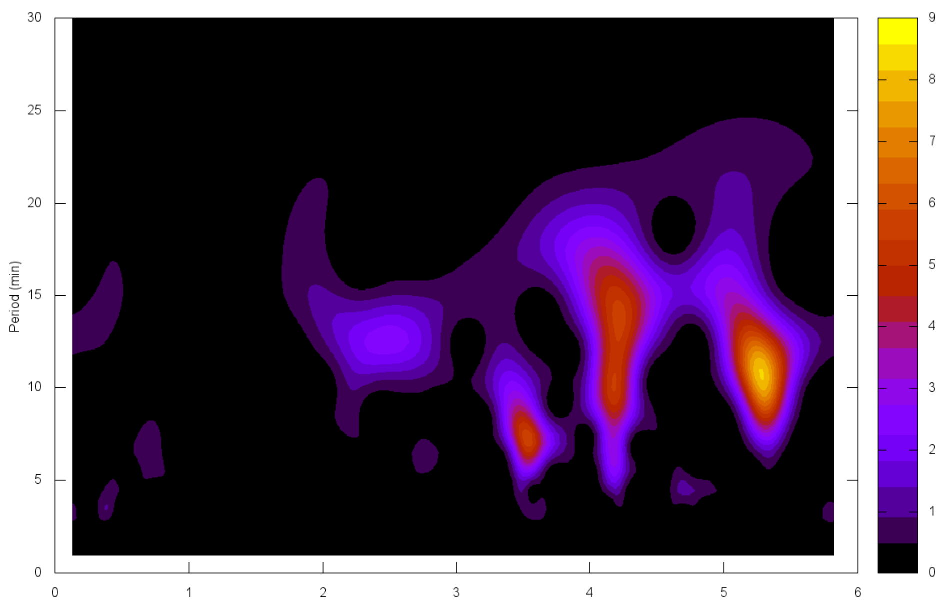

Figure 4.8 Wave-like activity from 0000-0600 EST, period (in minutes) and wave energy density (J/m^3) for January 25, 2010.

4.1 MODULATION OF SURFACE-ATMOSPHERE EXCHANGE BY WAVE ACTIVITY

The wave identified in the pressure signal for each night was used to determine the impact that waves have on uncorrected turbulence statistics and turbulent fluxes. The data that results is the wave(s) contribution to statistics and turbulent fluxes. For nights with multiple wave or wave-like events, only the time (2-hour window) during which the wave with the largest period or highest energy density was used to determine its contribution to the statistics and turbulent fluxes (see Tables 1 and 2). Table 1 contains 7 columns that include: 1) the day of the year, 2) the number of waves occurring between midnight and 6am that day, 3) the flux Ri for the 2-hour block of time during which the wave (selected from the pressure data) occurred, 4) the bulk Ri calculated for the 68 and 329m levels, 5) the periods (in minutes) of each wave, 6) the wave (with the largest period) inflation percentage / contribution to turbulent kinetic energy (TKE) at the 34m level, 7) the wave (with the largest period) contribution to turbulent kinetic energy at the 329m level. Because there was little difference between the 34m and 68m data, only the 34m and 329m data is presented here and compared. The asterisks in Tables 1 and 2 denote days with an anomalously high modulation of the turbulent signal percentages. That data and its possible causes were investigated. It was determined that the data was of excellent quality and thus the result was retained. However, no apparent cause for that anomaly was determined at this time. It is possible that this is attributed to the presence of thunderstorm activity in the area, acting as a trigger for the generation of large wave activity during that night. Weather data is required for further analysis to provide a useful clue to watch for such large events. We also have rejected all data for which rain at the site was present. In the case of the anomalously large degree of correction needed by the removal of the wave in the signal, it is likely that a large thunderstorm event occurring tens of miles away from the site would be retained as part of the dataset as there would be no rain locally at the site showing during those periods. Further study of the role of even remote thunderstorm activity in the generation of waves miles away appears warranted.

To calculate the inflation percentage the following equation is used:

$$\text{Error percentage} = (\text{'Original' flux} - \text{'dewaved' flux}) / \text{'Original' flux} \tag{4}$$

where the ‘original’ flux applies to the signal of the combined turbulence and wave components. The ‘dewaved’ flux denotes the flux for the signal after the wave component has been removed. This is the flux without the wave. The positive percentages mean that the measured ‘original’ value of a particular statistic or flux is higher than the ‘dewaved’ value and thus the wave increased / contributed to the statistic or flux positively. The negative percentages equate to a measured value that is lower than the signal without the wave component; therefore, the wave contributed to a decrease in the corresponding statistic or turbulent flux.

Table 1. Wave contribution to TKE for two contrasting seasons.

Day	Wave count	Ri_f	Ri_b	Wave periods (min)	34 m (%)	329 m (%)
				Winter 2009-10		
20091203	2	0.04	2.77	8, 12	11	0
20091205	4	1	32.4	8,9,15,17	9	4
20091212	4	0.5	26.8	5,7,9,10	8	1
20091231	2	1	27.5	4, 14	7	8
20090102	2	0.58	3.7	17, 21	55	50*
20100108	3	0.007	3.7	5, 8, 5	9	6
20100109	2	0.001	18.2	3, 14	8	0
20100125	4	1	40.1	9, 7, 11, 12, 14	11	3

20100130	2	0.75	24.6	12, 8	12	3
20100202	2	0.02	14	9,11	7	2
20100205	2	0.31	35.2	7, 12	5	2
20100213	1	0.009	4.75	12	10	3
				Summer 2009		
20090606	1	4.1	36.93	8	5	1
20090608	1	2.7	39.59	16	1	25*
20090806	2	1	10.45	5,9	7	14
20090812	1	0.003	4.11	12	1	2
20090813	4	1	9.29	5,5,8,15	3	4
20090815	3	1.2	12.78	3,4,5	4	8
20090821	2	2.5	29.4	8,10	4	12
20090822	1	0.003	3.4	3	<1	5
20090830	1	0.017	8.5	11	1	4
20090831	3	1	11.5	10,13, 22	1	10

During the winter, nights characterized as turbulent had a higher frequency of events and waves with longer periods than during a summer turbulent night. This is because the atmosphere is generally more stable owing to the presence of strong thermal inversions. There was only one night with only one wave event in the winter, as shown in Table 1, while for the summer, half of the nights had only one wave event. Water vapor and carbon dioxide fluxes, momentum and heat scalars (see Appendix A) as well as TKE flux, TKE, and friction velocity (u_*) were calculated in this study and shown in Tables 1 and 2.

Table 2 contains 5 columns that include: 1) the day of the year, 2) the wave (with the largest period) error percentage / contribution to turbulent kinetic energy flux at the 34m level, 3) the wave (with the largest period) contribution (percentage) to turbulent kinetic energy flux at the 329m level, 4) the wave (with the largest period) error percentage of u_* at the 34m level, 5) the wave (with the largest period) contribution (percentage) to u_* at the 329m level. The winter data precedes the summer data in each of the tables. Since the evaluation of the presence of waves in nighttime conditions appear to have a minor impact on scalar fluxes of CO_2 and H_2O fluxes at 34m and 329m, they are not discussed in the body of the text and the reader is referred to Appendix A.

Table 2. Wave contribution to TKE flux and U_* for two contrasting seasons.

Day	34m (%)	329m (%)	34 m (%)	329 m (%)
		Winter 2009-10		
20091203	2	5	5	0
20091205	1	1	2	4
20091212	4	7	1	1
20091231	2	4	4	8
20090102	2	1	3	2
20100108	5	1	5	6
20100109	1	1	8	0
20100125	4	1	1	3
20100130	1	2	2	3
20100202	3	1	2	1
20100205	5	5	5	2

20100213	1	1	3	1
		Summer 2009		
20090606	1	8	5	1
20090608	1	1	1	2
20090806	2	9	7	4
20090812	3	8	3	2
20090813	4	5	1	4
20090815	3	1	4	8
20090821	2	3	4	5
20090822	1	8	<1	5
20090830	1	7	1	3
20090831	1	1	3	7

From Table 1, two special cases appear to have anomalously high contributions to TKE at the 329m level. June 8th 2009 and a second January 2nd 2010 show differences in activity, with June 8th having one large amplitude and high density event while Jan. 2nd had two. The pressure perturbations were much higher for January 2nd than June 8th. The average periods of the wave-like events were 16 minutes (one single event) for June and 19 minutes for January. Both nights had high wave-like activity during the six-hour time period and across the wide range of periods. The Ri_b was 39.59 and January 2nd had a Ri_b of 3.7. Fluxes and statistics varied with height for the 'dewaved' and original signals. On June 8th the errors for TKE at 329m the value was a staggering 25%, while at the 34m level error was roughly 1%. In contrast, the night of January 2nd had errors around 55% at 34m and 50% at the 329m level.

For June 8, 2009, the wave corresponded to a decrease in friction velocity at the time of its occurrence (about 2 am) at both the 34m and 329m levels (Figures 4.9 and 4.10). Similarly, the TKE flux decreased at both levels (see Figures 4.11 and 4.12). At the time of the wave, the original values are higher than the 'dewaved' signal by ~42% at 34m and ~50% at 329m.

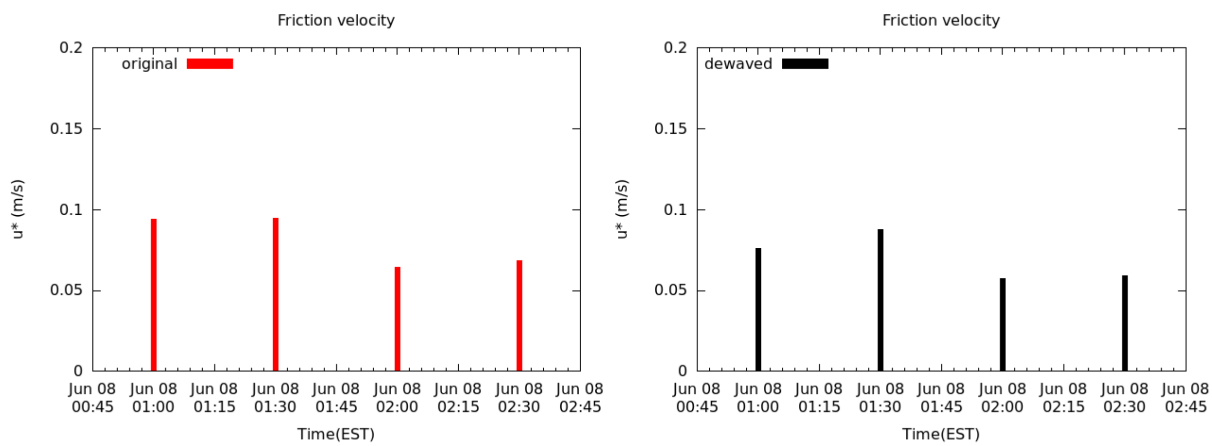

Figure 4.9 'Original' and 'dewaved' U* for June 8, 2009 at the 34m level.

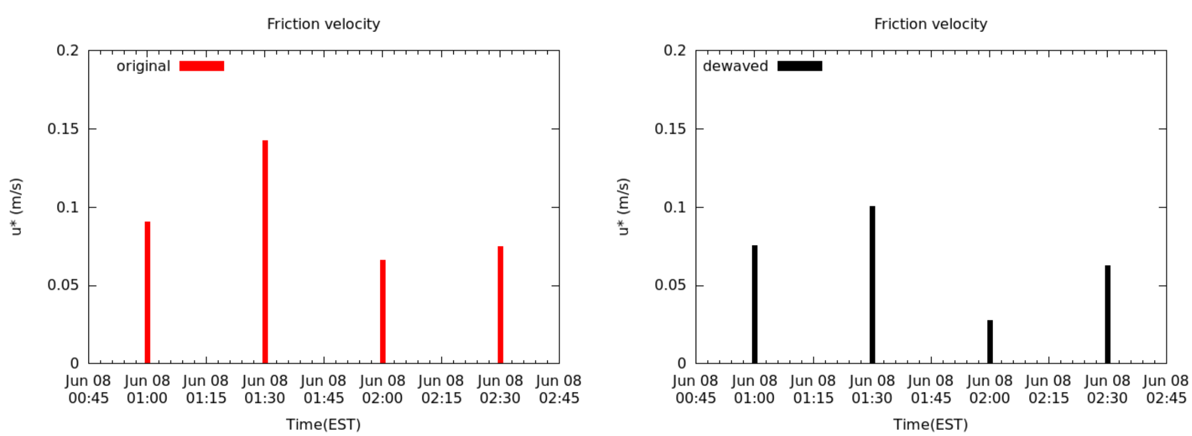

Figure 4.10 'Original' and 'dewaved' U* for June 8, 2009 at the 329m level.

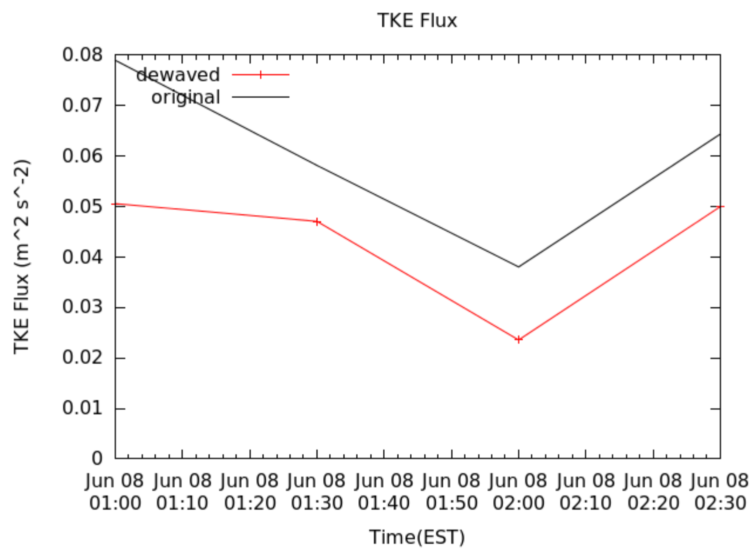

Figure 4.11 'Original' and 'dewaved' TKE flux for June 8, 2009 at the 34m level.

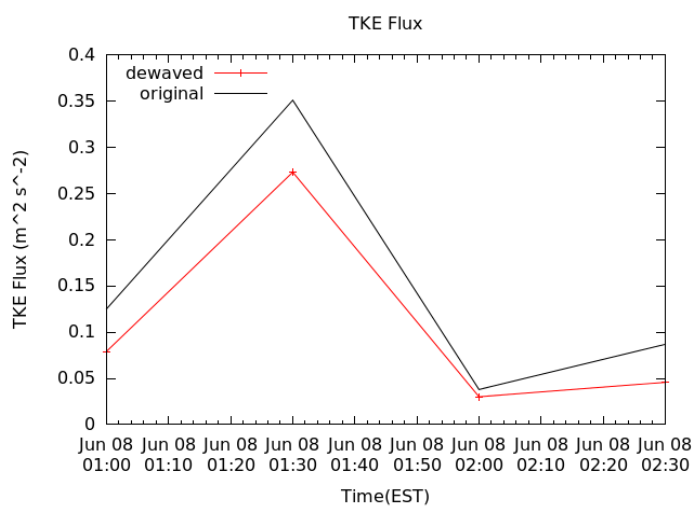

Figure 4.12 'Original' and 'dewaved' TKE flux for June 8, 2009 at the 329m level.

August 12, 2009, had a large-period wave that corresponded to a decrease in friction velocity at the time of its occurrence (about 5 am) at the 34m level and 329m level (see Figures 4.13 and 4.14). The TKE flux (Figures 4.15 and 4.16) decreased at both 34 and 329m. At the time of the wave, the original values are consistently higher that the ‘dewaved’ signal, so the wave is contributing to the friction velocity and TKE flux.

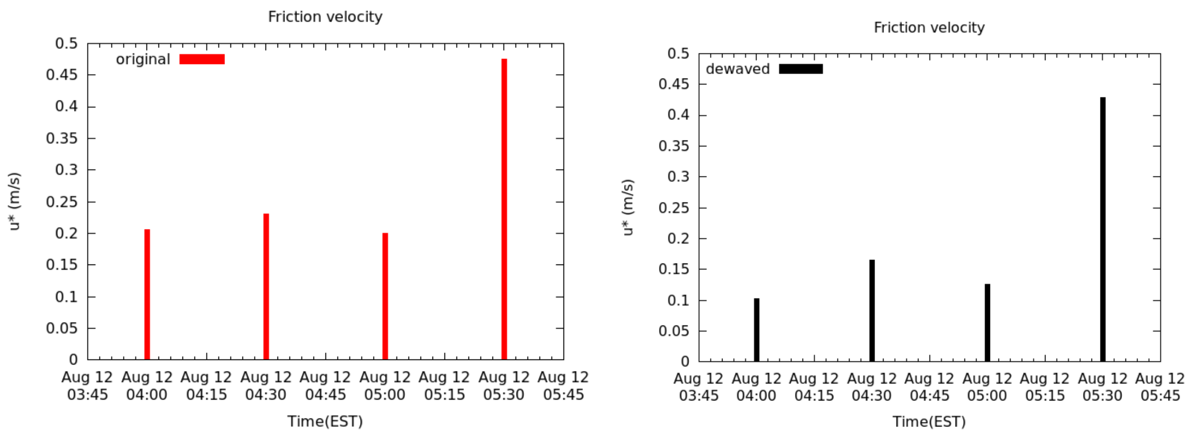

Figure 4.13 ‘Original’ and ‘dewaved’ U_* for August 12, 2009 at the 34m level.

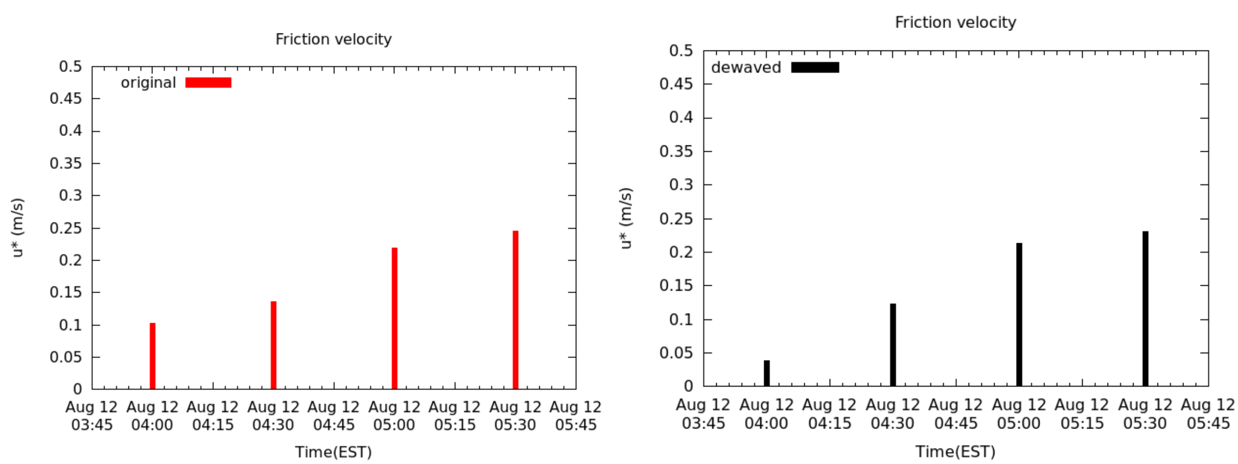

Figure 4.14 ‘Original’ and ‘dewaved’ U_* for August 12, 2009 at the 329m level.

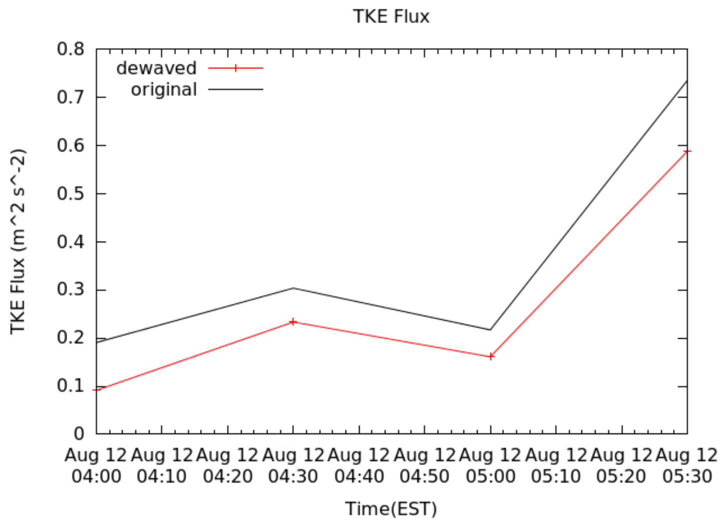

Figure 4.15 ‘Original’ and ‘dewaved’ TKE flux for August 12, 2009 at the 34m level.

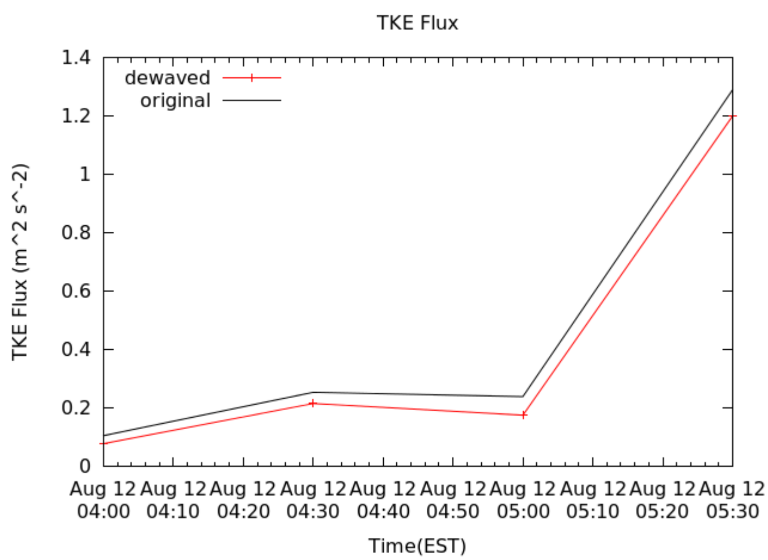

Figure 4.16 ‘Original’ and ‘dewaved’ TKE flux for August 12, 2009 at the 329m level.

On January 2, 2010, a wave between 1 and 2 am corresponded to a gradual decrease in friction velocity for the duration of its occurrence at the 34m level and a gradual increase 329m level (see Figures 4.17 and 4.18). The TKE flux (Figures 4.19 and 4.20) showed the same pattern of change as the friction velocity. At the time of the wave, the original values are consistently higher that the 'dewaved' signal, almost three times as much at 34m and twice as much at the 329m level, so the wave is significantly contributing to the friction velocity and TKE flux on this morning. For January 25, 2010, three waves corresponded to a change in friction velocity at the time of occurrence, but the two latest waves (at ~4:45 and ~5:10 am) corresponded to increases at the 34m level and decreases at the 329m level (Figures 4.21 and 4.22). The TKE flux increased at both the 34m and 329m levels (see Figures 4.23 and 4.24). At the time of the wave, the original values are much higher that the 'dewaved' signal at both levels, similar to January 2nd.

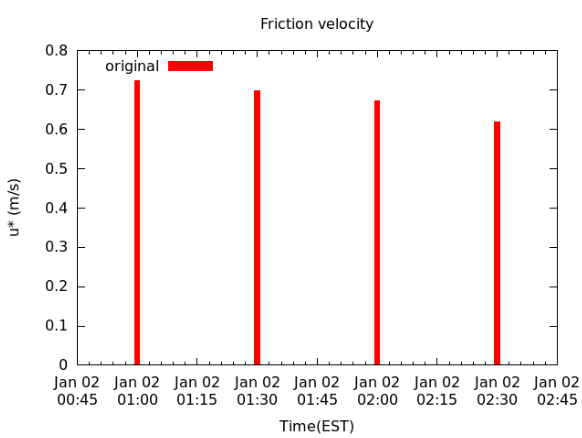

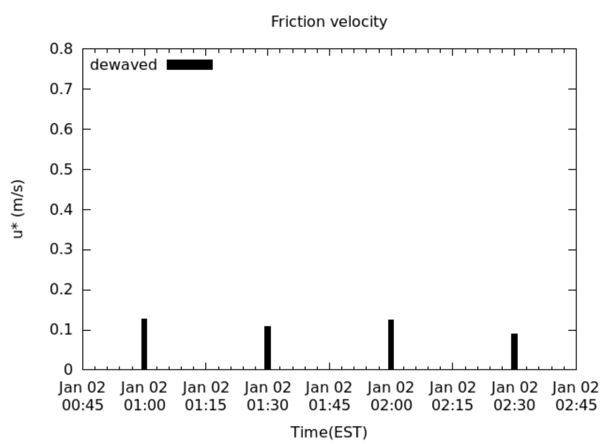

Figure 4.17 'Original' and 'dewaved' U_* for January 2, 2010 at the 34m level.

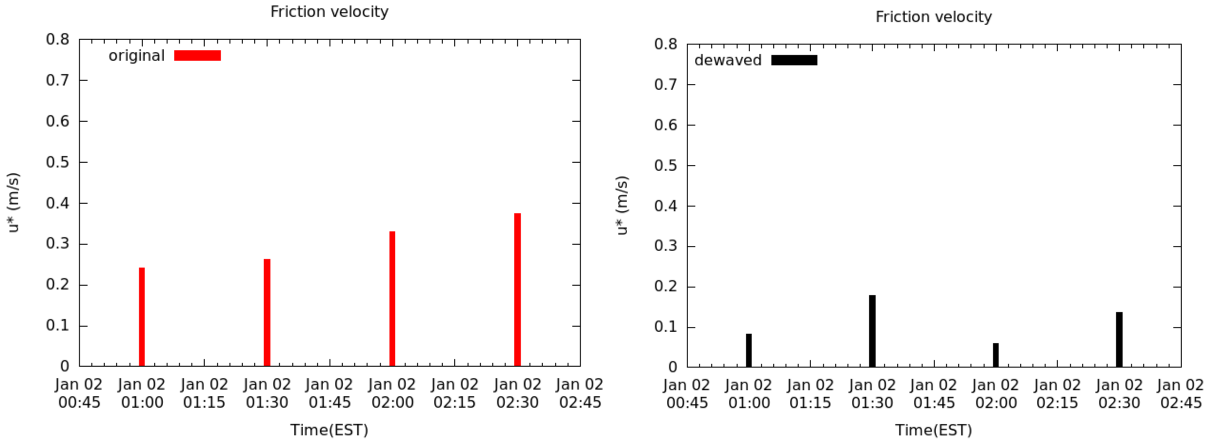

Figure 4.18 ‘Original’ and ‘dewaved’ U_* for January 2, 2010 at the 329m level.

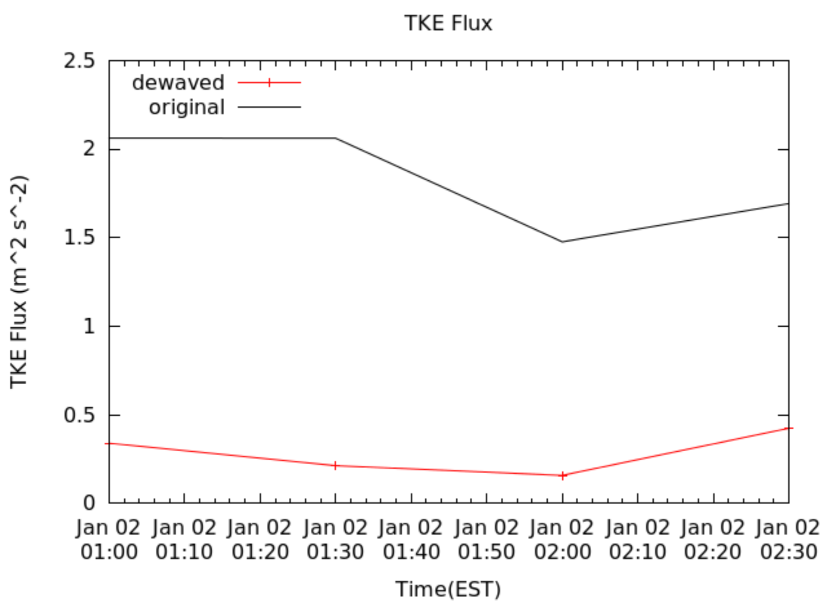

Figure 4.19 ‘Original’ and ‘dewaved’ TKE flux for January 2, 2010 at the 34m level.

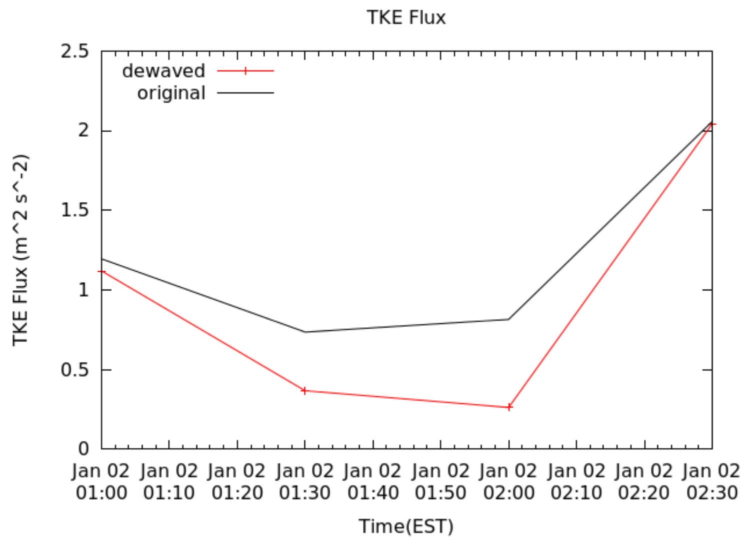

Figure 4.20 'Original' and 'dewaved' TKE flux for January 2, 2010 at the 329m level.

On average in winter, wave activity contributes 12% to TKE at 34m and 6% at 329m and only 2% to TKE fluxes at 34m and 3% at 329m on average. For u_*, there is a 3% contribution at 34m and 2% at 329m. On average during summer, wave activity contributes 8% at 329m and 3% at 34m to TKE and only 2% to TKE fluxes at 34m and 5% at 329m. There was a 3% contribution at 34m and 4% at 329m for u_*.

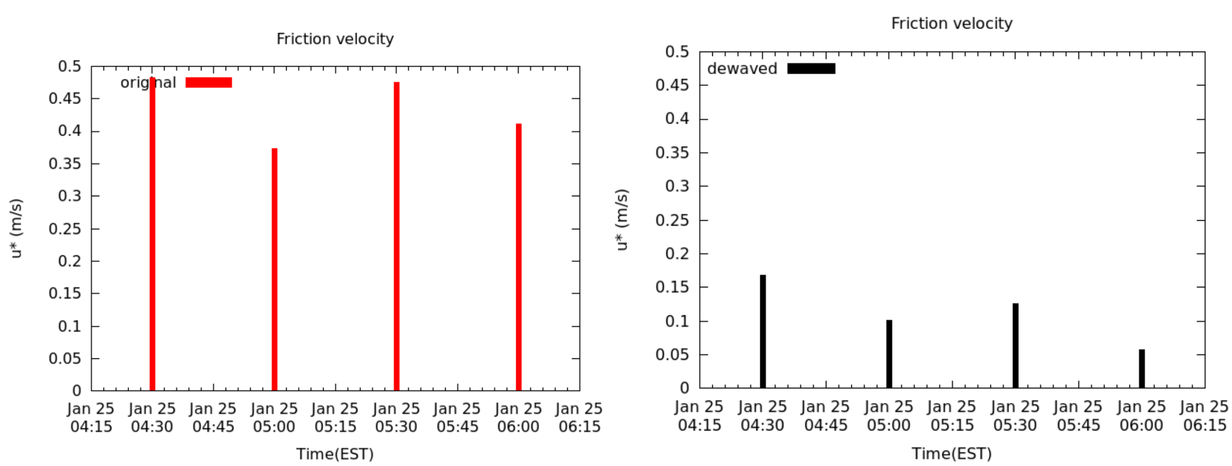

Figure 4.21 'Original' and 'dewaved' U_* for January 25, 2010 at the 34m level.

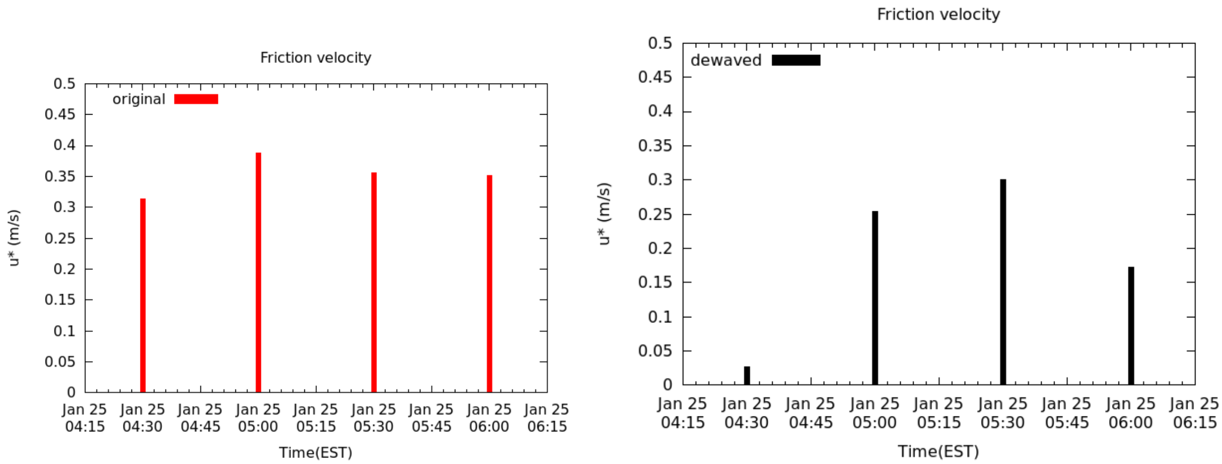

Figure 4.22 'Original' and 'dewaved' U* for January 25, 2010 at the 329m level.

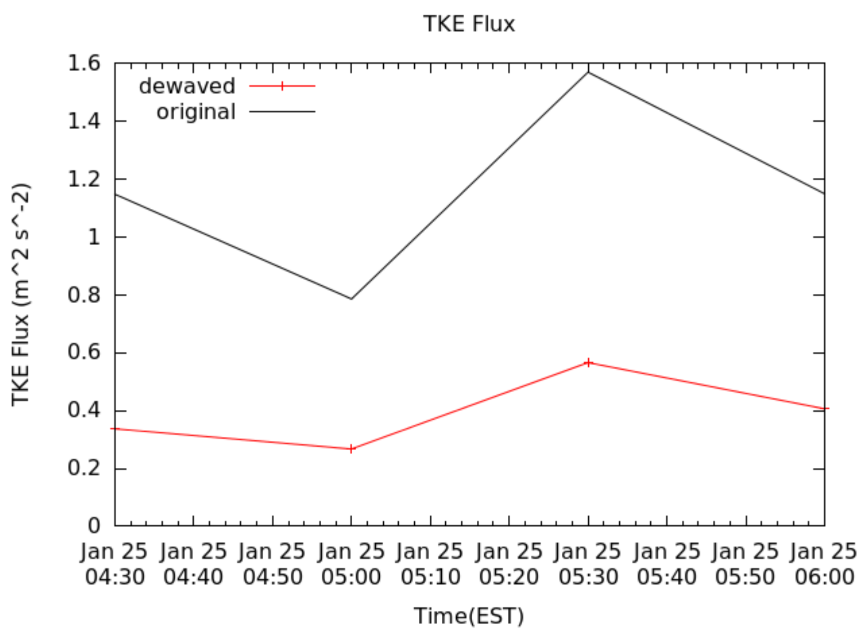

Figure 4.23 'Original' and 'dewaved' TKE flux for January 25, 2010 at the 34m level.

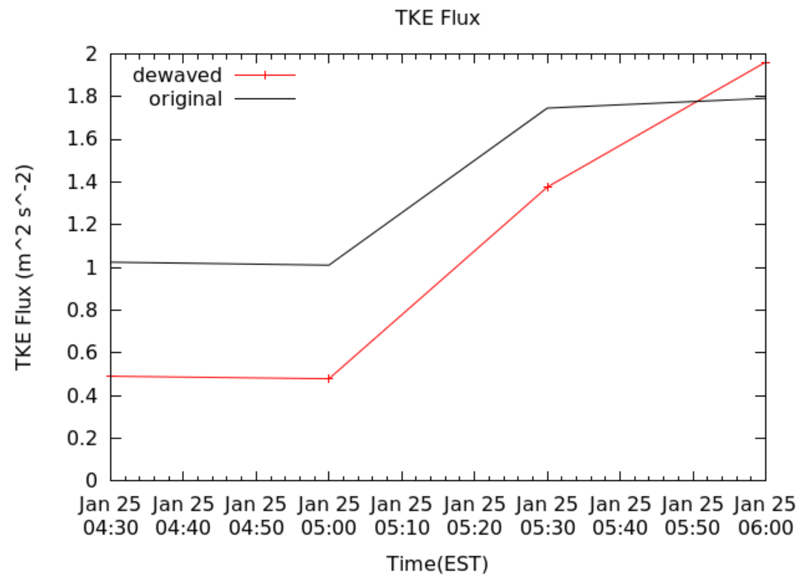

Figure 4.24 'Original' and 'dewaved' TKE flux for January 25, 2010 at the 329m level.

5 DISCUSSION

Wave propagation shown at both levels for selected days was shown. The turbulence statistics consistently shows errors when the averaging time for fluxes is longer than the wave period. With the dataset used in the present analysis, the degree of errors in the turbulent kinetic energy was highly variable across seasons. The data analyzed suggest considerable variability in the impact of waves from day to day. As consistent with the atmospheric conditions required to sustain wave activity, wave thrive during calm, quiescent stable nighttime conditions while they are not sustained and play only a minor role in windier, more neutral nighttime conditions.

Based on the present analysis, at the lower level near the ground where most of the eddy-flux systems are generally located, waves propagating during the winter were more frequent with longer periods and higher intensity than those in spring in nighttime conditions. This is likely a result of stronger stable stratification near the surface.

There is a marginal impact of waves on statistics on summer nights. More specifically, there are large contributions from high-frequency events with mild stability. As mentioned earlier, when multiple waves of different frequencies were embedded in the flux/turbulence signal simultaneously, the analysis focused on the wave with the largest period.

Turbulence statistics in the presence of a wave event vary with height in the stable nocturnal boundary layer and the degree of their impact varied considerably with height and with season. At the 34m level, there appears to be a consistent pattern of heightened wave activity in the winter when compared with summer. That may be a reflection of the fact that strong thermal inversion by the surface during the winter enhances stability which in turn acts to support the presence of waves.

The present evaluation may not be necessary for waves to be removed from turbulence when only scalar fluxes are sought. Similarly, errors may be small for turbulence statistics when averaging periods are shorter than the respective period. If this is assessed initially, then calculations used to remove wave-linked errors can be avoided.

This study evaluates, for the first time, the impact of both height and time of year on wave activity with their subsequent impact on turbulent eddy-flux data and turbulence statistics. It detects the periods and frequency of waves present within a 30-min typical averaging time used traditionally in flux calculations. It then quantifies the degree of error in turbulence statistics and fluxes that arise from the presence of the waves. The impact is greatest near the surface where the atmosphere is most stable during the winter, while the impact is great in the boundary layer during the summer. It has been discussed that strong thermal inversions present wintertime lead to strong atmospheric stability providing the conditions necessary to support wave activity in the nocturnal boundary layer.

The present study demonstrates that the frequency and intensity of large-amplitude pressure events increased drastically during the winter months. This finding is consistent with preliminary case study presented by Durden et al. (2013), who used an ensemble of monthly standard deviation averages across a year to 'pinpoint' the patterns in stability.

Results presented here suggest that the calculation of statistics and fluxes at a single height is insufficient to infer about wave activity and wave-induced errors in flux and turbulence statistics prevailing conditions at other levels, or for a different location at the same level as what has been looked into with the present study. Considering the spatial and temporal variability of waves in the atmosphere, the degree of resulting errors in turbulence statistics and errors in the turbulent fluxes is also likely to be very site-specific. Factors such as land-sea breezes, mountain ranges, atmospheric thermal contrasts from two adjacent contrasting surface properties, and the presence of even thunderstorm activity even occurring at tens of miles away from the flux site, all are factors which are likely to modulate the presence of those waves and their impact on the local turbulence and turbulence flux characteristics.

For nights with significant levels of turbulence, turbulence calculations were less enhanced by wave or wave-like events compared to nights with little to no turbulence (i.e. calm nights lead to more waves and thus more errors in statistics). In relation to turbulent flow, the weakly stable boundary layer develops under a different, more disturbed pattern or mechanism than its ‘very stable’ counterpart, resulting in a continuous and weak turbulent stable layer at the surface (Salmond and McKendry, 2005; Mahrt et al., 1998).

Past research has found that a significant portion of the vertical transport of heat and moisture in the lower very stable nocturnal boundary layer occurs in intermittent bursts and often and sporadically throughout the night (Salmond and McKendry, 2005; Mahrt, 1998). The large turbulent kinetic energy error seen on the 8th of June of 25% at a 329m level appeared to be an anomaly. The June 8th anomaly and the pattern of unusually large impact of the wave on the turbulence statistics at the 329m level during the summer months could not be definitively explained from these findings. The data was analyzed a second time for quality and found to be excellent. Therefore, this large error arising from the presence of the waves in the signal may be attributed to a phenomenon such as that of thunderstorm activity taking place miles away from the eddy-flux system: this is because the data with rain on the eddy-flux system was eliminated as part of the signal processing to preserve only high-quality data, such wave impact generated by thunderstorms would originate miles from the site. Several different occurrences including a maximum wind speed at or near the 329m level (not shown), changes in wind speed or wind direction, some vertical transport of energy into the layer that coincided with the wave-event, and/or some other unidentifiable mechanism could have helped in triggering the presence of important wave activity. To this date, there is a notable paucity of data on the subject.

6 CONCLUSIONS

Data collected from a campaign at the Savannah River Site near Aiken, South Carolina in 2009 and 2010 were used to evaluate the effect of wavelike disturbances on turbulence and flux statistics obtained from an eddy-flux system over approximately 151 nights. Attention was given to the acquisition and analysis of a dataset that spans multiple months across two contrasting seasons of summer and winter respectively. The study also evaluated the frequency of occurrence of wave activity with two contrasting levels. The premise was made that strong thermal stratification enhances and supports wave activity and thus, as our results show, the presence of waves and their subsequent impact on turbulence statistics is largest in the winter and near the ground where the atmosphere is most stable. In general, all other conditions aside, the presence and propagation of waves increases with distance from the ground. However, this study finds that this pattern appears to hold only for summer months where inversions are weakest. This may explain the apparent lack of consistency in the presence of waves and their respective impact when both heights and seasons are taken into account.

The present study shows that large amplitude wave-like events occurred on ~15% of the 151 nights studied (all days considered). The analysis only considered waves that are completely contained within the 30-min averaging period, characteristic of standard eddy-flux systems data analysis packages. Waves which were present and which were smaller and appear simultaneously with another larger wave within the 30-min window had a period smaller than the largest wave were not considered. Their inclusion would contribute to increase significantly the total impact of waves on fluxes as can be inferred from the evaluation of the Tables presented in the Results section

Without proper filtering, overestimated turbulence statistics of up to 55% for TKE at the 34m level and 50% for TKE at the 329m level and erroneous flux calculations may occur on calm, quiescent nights. Although these large values are a singular occurrence, the data shows that significant modulation of turbulence statistics by wave activity is present for the turbulence kinetic energy and the turbulent kinetic energy fluxes. Such result is important to atmospheric modelers and boundary-layer modelers. From the findings here, in stable conditions the wave contribution is a much larger percentage; thus, the impact appears relatively more significant. As expected and as shown in the present work with the help of the stability parameter Ri, waves are most present and their impact greatest when the atmosphere is stable.

The evaluation of the presence of the wave modulation on turbulent CO_2 and H_2O fluxes was found to be negligible and the readers is invited to examine the Appendix if more information is sought on the matter.

Results from this study suggest that it is important to identify wave activity and remove them when calculating turbulence parameters and turbulent fluxes are sought particularly in the presence of strong thermal stratification close to the ground or at higher levels otherwise.

Future work could consist of determining the year to year variability of wave characteristics and their impact on turbulence statistics and fluxes across multiple years; this could help provide much needed insight on the interannual variability of these waves with the resulting impact on fluxes. In addition, the variability across flux sites should be investigated. The present dataset is the first and by far the largest dataset which comprises a combination of flux measurements taken at very large differences in vertical levels. It is also possibly the only study anywhere (outside the preliminary case study by Durden et al. (2012) which combines both eddy-flux data collected coincidentally with the presence of a microbarograph at the surface. A larger dataset would provide added flexibility and robustness in the determination of the impact of waves on eddy-flux data. The impact of a longer averaging time and a determination of the sensitivity of the wave detection algorithm to varying standard deviations of the pressure time series is recommended.

REFERENCES

Chimonas G., (1999) Steps, waves, and turbulence in the stably stratified planetary boundary layer. Boundary-Layer Meteorol. 90, 397–421.

Collineau S., Brunet Y. (1993a) Detection of turbulent coherent motions in a forest canopy, Part I: Wavelet analysis. Boundary-Layer Meteorol. 65, 357–379.

Collineau S., Brunet Y. (1993b) Detection of turbulent coherent motions in a forest canopy, Part II: Time-scales and conditional averages. Boundary-Layer Meteorol. 66, 49–73.

Durden D., Nappo C., Leclerc M., Duarte H., Zhang G., Parker M., Kurzeja R. (2013) On the impact of wave-like disturbances on turbulent fluxes and turbulence statistics in nighttime conditions: a case study. Biogeosciences. 10, 8433-8443.

Einaudi, F. and Finnigan, J. J. (1981) The interaction between an internal gravity wave and the planetary boundary Layer. Part I: The Linear Analysis. Q. J. Roy. Meteor. Soc. 107, 793-806.

Einaudi, F. and Finnigan, J.J. (1993) Wave-turbulence dynamics in the stably stratified boundary layer. Journal of Atmospheric Sci. 50, 1841-1864.

Einaudi, F., Finnigan, J.J., and Fua, D. (1984) Gravity wave turbulence interaction in the presence of a critical level. Journal of Atmospheric Sci. 41, 661-667.

Farge M. (1992) Wavelet transforms and their applications to turbulence. Ann Rev Fluid Mech. 24, 395–457.

Hauf, T., Finke, U., Neisser, J., Bull, G., and Stangenberg, J.-G. (1996) A ground-based network for atmospheric pressure fluctuations. Journal of Atmospheric and Oceanic Tech. 13, 1001-1023.

Karipot, A., M.Y. Leclerc, G. Zhang, T. Martin, G. Starr, D. Hollinger, L.E. Hipps, McCaughey, D. J. Anderson and G. R. Hendrey. (2006). Nocturnal CO2 Exchange Over a Tall Forest Canopy Associated with Intermittent Low-Level Jet Activity. Journal of Theoretical and Applied Climatol. 85, 243-248.

Mahrt, L. (2009) Characteristics of submeso winds in the stable boundary layer. Boundary-Layer Meteorol. 130, 1-14.

Mathieu, N., I. B. Strachan, M. Y. Leclerc, A. Karipot, and E. Pattey, (2005) Role of low-level jets and boundary-layer properties on the NBL budget technique. Agricultural and Forest Meteorol. 135, 35-43.

Nappo, C. J., D. R. Miller, and A. L. Hiscox, (2008) Wave-modified flux and plume dispersion in the stable boundary layer. Boundary-Layer Meteorol. 129, 211-223.

Nappo, C. J., A. L. Hiscox and D. R. Miller, (2010) A Note on Turbulence Stationarity and Wind Persistence within the Stable Planetary Boundary Layer. Boundary-Layer Meteorol. 136, 165-174.

Salmond, J. (2005) Wavelet analysis of intermittent turbulence in a very stable nocturnal boundary layer: Implications for the vertical mixing of ozone. Boundary-Layer Meteorol. 114, 463–488.

Salmond, J. and McKendry, I. (2005) A review of turbulence in the very stable nocturnal boundary layer and its implications for air quality. Progress in Physical Geo. 29, 171–188.

Torrence C., Compo G.P. (1998) A practical guide to wavelet analysis. Bulletin of American Meteorological Soc. 79, 61–78.

Turner B.J., Leclerc M.Y. (1994) Conditional sampling of coherent structures in atmospheric turbulence using the wavelet transform. J Atmos Ocean Tech. 11, 205-209.

Turner B.J., Leclerc M.Y., Gauthier M., Moore K.E., Fitzjaarald D.R. (1994) Identification of turbulence structures above a forest canopy using the wavelet transform. J Geophys Research. 99, 1919–1926.

Van Gorsel E., Delpierre N., Leuning R., Black A., Munger J.W., Wofsy S., Aubinet M., Feigenwinter C., Beringer J., Bonal D., Chen B., Chen J., Clement R. (2009) Estimating nocturnal ecosystem respiration from the vertical turbulent flux and change in storage of CO_2. Agricultural and Forest Meteorol. 149, 1919–1930.

Van Gorsel E., Harman I.N., Finnigan, J.J., Leuning R. (2011) Decoupling of airflow above and in plant canopies and gravity waves affect micrometeorology estimates of net scalar exchange. Agricultural and Forest Meteorol. 151, 927–933.

Van Gorsel E., Berni J., Briggs P., Cabello-Leblic A., Chasmer L., Cleugh H.A., Hacker J., Hantson S., Haverd V., Hughes D., Hopkinson C., Keith H., Kljun N., Leuning R., Yebra M., Zegelin S.(2013) Primary and secondary effects of climate variability on net ecosystem carbon exchange in an evergreen eucalyptus forest. Agricultural and Forest Meteorol. 182-183, 248–256.

Viana R.L., Lopes S.R., Szezech J.D., Caldas I.L. (2012) Synchronization of chaos and the transition to wave turbulence. International Journal of Bifurcation and Chaos, 22, 1–9.

Yi C. (2009) Instability analysis of terrain-induced canopy flows. Journal of the Atmospheric Sci. 66, 2134-2142.

Zeri M., Sa L.D.A. (2011) Horizontal and vertical turbulent fluxes forced by a gravity wave event in the nocturnal atmospheric surface layer over the Amazon forest. Boundary-Layer Meteorol. 138, 413-431.

Zhang G., Thomas C., Leclerc M.Y., Karipot A., Foken T. (2007) On the effect of clearcuts on turbulence structure above forest canopy. Theoretical and Applied Climatol. 88, 133-137.

Zhu J., Zhang J.A., Masters F.J. (2010) Wavelet analyses of turbulence in the hurricane surface layer during landfalls. Journal of the Atmospheric Sci. 67, 3793–3805.

APPENDIX

Table A. Wave with largest period contribution to $\overline{w'T'}$ and $\overline{w'U'}$, respectively, at 34 and 329m levels for two contrasting seasons.

Day	34 m (%)	329 m (%)	34 m (%)	329 m (%)
Winter 2009-10				
20091203	0	<1	-1	1
20091205	1	-1	-1	-1
20091212	-1	1	5	1
20091231	-1	1	2	1
20090102	1	2	1	5
20100108	2	0	5	0
20100109	<1	2	1	3
20100125	<1	1	2	3
20100130	5	1	3	1
20100202	1	1	-1	-1
20100205	2	-1	1	1
20100213	1	-1	4	1
Summer 2009				
20090606	-1	-1	-1	1
20090608	-1	1	-2	3
20090806	5	1	-1	2
20090812	4	-1	1	2
20090813	2	-1	3	4
20090815	1	2	1	1

20090821	3	2	4	1
20090822	-1	5	1	4
20090830	2	3	-1	3
20090831	5	0	1	2

Table A shows the heat and momentum scalars for all the days in winter and summer.

Table B. Wave with largest period contribution to CO_2 and H_2O fluxes at 34 and 329m levels for two contrasting seasons.

Day	34 m (%)	329 m (%)	34 m (%)	329 m (%)
		Winter 2009-10		
20091203	0	<1	-1	1
20091205	1	-1	-1	-1
20091212	-1	1	5	1
20091231	-1	1	2	1
20090102	1	2	1	5
20100108	2	0	5	0
20100109	<1	2	1	3
20100125	<1	1	2	3
20100130	5	1	3	1
20100202	1	1	-1	-1
20100205	2	-1	1	1
20100213	1	-1	4	1
		Summer 2009		
20090606	-3	3	<1	0

20090608	-1	1	-2	1
20090806	5	1	-1	2
20090812	4	-1	1	2
20090813	7	2	<1	4
20090815	1	2	<1	1
20090821	3	5	1	1
20090822	-1	-1	<1	2
20090830	1	2	1	3
20090831	3	0	1	1

Table B shows the water vapor and carbon dioxide fluxes for all the days in winter and summer.